

Ion-Water Cluster Molecular Dynamics Using a Semiempirical Intermolecular Potential

Noelia Faginas-Lago¹(✉), Margarita Alberti²,
Antonio Laganà¹, and Andrea Lombardi¹

¹ Dipartimento di Chimica, Biologia e Biotecnologie,
Università di Perugia, Perugia, Italy
piovro@gmail.com

² IQTCUB, Departament de Química Física,
Universitat de Barcelona, Barcelona, Spain

Abstract. Classical Molecular Dynamics (MD) simulations have been performed to describe structural and dynamical properties of the water clusters forming around the Na^+ and K^+ . The dynamics of K^+ and Na^+ was investigated for small water clusters $[\text{K}(\text{H}_2\text{O})_n]^+$ and $[\text{Na}(\text{H}_2\text{O})_n]^+$ ($n = 3 - 8$), isolated in gas phase following the structure transformation through isomerizations between the accessible energy minima. The extent to which a classical molecular simulation accurately predicts properties depends on the quality of the force field used to model the interactions in the fluid. This has been explored by exploiting the flexibility of the Improved Lennard-Jones (ILJ) function in describing the long-range interaction of ionic water systems.

Keywords: Molecular Dynamics · Empirical potential energy surface · Ion-water clusters · DL.POLY

1 Introduction

Aqueous solvation of metal ions plays a central role in the chemical mechanisms of biological signaling, in the bioavailability of toxic elements within the environment, in the design of new catalysts and in extraction processes, as well as in many phenomena relevant to technology [1–6]. For example, a problem of current interest focuses on the selectivity of biological ion channels; it seems clear that the selective transport of K^+ relative to Na^+ ions in potassium channels [7–9] depends on details of the ion hydration structure that might differ for K^+ relative to Na^+ ions.

A key feature of solvation is the structural organization of water about the ion, which includes the positions of the oxygen atoms and the influence of the ion upon the water's H-bonding network [10].

A fingerprint of the structure of these systems is the coordination number of the ion in liquid water, a number that in terms of the organization of water around the ion as spherical shells, determines how many water molecules are contained in each of them [11].

The measurements of this property of ions in water is to date still controversial, due to uncertainties in related experimental measurements and in theoretical simulations. Experimental efforts to define the hydration structure of K^+ , by means of neutron diffraction [12,13] and extended X-ray absorption fine structure spectroscopy (EXAFS) experiments [14], gave coordination number values varying between 4 and 8 [15]. Also, for Na^+ ion, neutron diffraction [16,17] and spectroscopic [18] methods produce a hydration number ranging between 4 and 6 [19]. To the end of understanding such data one has to account accurately for ion-water and water-water interactions. For example, the complex interplay of ion-water and water-water interactions is the mechanism ensuring the functioning of sodium-potassium pump of living cells [20]. In this respect, fundamental is the understanding of the intermolecular interactions, and the modeling of competing non-covalent forces.

The main goal of this work goes, indeed, in that direction by investigating the geometry optimization and binding energy of clusters $[Na(H_2O)_n]^+$ and $[K(H_2O)_n]^+$ (where $n=3-8$) using classical Molecular Dynamics assisted by ab initio electronic structure calculations [21]. These simulations were analyzed with respect to structural parameters such as radial distribution functions and coordination number distributions.

The original potential model used here is based on a formulation of the non electrostatic approach to the intermolecular interaction that exploits the decomposition of the molecular polarisability [22] into effective components associated with atoms, bonds or groups of atoms of the involved molecules. This type of contribution to the intermolecular energy was already applied in the past to the investigation of several neutral [23–31] and ionic [32–34] systems, often involving weak interactions [23,35], difficult to calculate. The adequacy of such potential energy functions to describe several intermolecular systems was proved by comparing energy and geometry predictions at several configurations with ab initio calculations. In particular, the study of the alkali ion systems [36,37] was useful to quantify the role, that chemical contributions play in such aggregates.

The paper is organized as follows: in Sec. 2, we outline the construction of the potential energy function. We give in Sec. 3 the details of the Molecular Dynamics simulations. Results are presented in Sec. 4 and concluding remarks are given in Sec. 5.

2 Potential Energy Surface

To obtain a potential energy surface suitable for running MD simulations, the $M^+-(H_2O)_n$ ($M^+=K^+, Na^+$) intermolecular interaction energy, V , is decomposed in terms of ion-molecule and molecule-molecule pair contributions, as follows:

$$\begin{aligned}
 V = & \sum_{k=1}^n V_{M^+-(H_2O)_k} \\
 & + \sum_{k=1}^{n-1} \sum_{j>k}^n V_{(H_2O)_k-(H_2O)_j}
 \end{aligned}
 \tag{1}$$

where n is the total number of water molecules and all intermolecular terms in Eq. 1 include both electrostatic and non electrostatic contributions. The non electrostatic contributions to the sum of Eq. 1 are evaluated by assigning a value of polarizability (denoted hereinafter as α) to the two interacting centers of each term, so as to account for both the strength of the induced dipoles (the attraction) and the average atomic and molecular sizes (exchange - repulsion). A detailed account of the use of polarizabilities for this purpose is given in Refs. [24, 38] and references therein. As it has been mentioned above, in this case the H_2O molecule has a low value of polarizability and the quantities α_{M^+} ($M^+ = K^+, Na^+$) and α_{H_2O} have neither been decomposed as a sum of contributions nor displaced with respect to the ion and molecule positions, meaning that, besides K^+ and Na^+ , also H_2O is considered in our model as a single interaction centre placed coincident with the O atom and bearing the total value of α_{H_2O} . This finds its rationale in the fact, that a model considering the presence of more interaction centres (i.e. bond and effective atom polarisabilities) leads to about the same structural and energetic properties of the ion-water interaction [34, 39].

The model, however, could be improved by taking into account, if needed, the anisotropy in water-water interaction by explicitly considering the water molecule bonds as interacting centres. The pairwise interaction contributions between centres placed on different molecules, are described by means of the Improved Lennard Jones (ILJ) function V_{ILJ} [40, 41],

$$V_{ILJ} = \varepsilon \left[\frac{m}{n(r) - m} \left(\frac{r_0}{r} \right)^{n(r)} - \frac{n(r)}{n(r) - m} \left(\frac{r_0}{r} \right)^m \right]
 \tag{2}$$

with

$$n(r) = \beta + 4.0 \left(\frac{r}{r_0} \right)^2
 \tag{3}$$

used to describe other systems interacting with water [42].

The reliability of the ILJ function given above has been validated by reproducing the highly accurate scattering data obtained from experiments performed under high angular and energy resolution conditions [41]. Further reliability tests were performed by comparing calculated vibrational spacings with experimental values and calculated interaction energies at short-range with those obtained from the inversion of gaseous transport properties. The analysis, extended also to systems involving ions, suggests that the ILJ potential model can be used to estimate the behaviour of a variety of systems and can help to assess the different role of the leading interaction components [43].

In Eq. 2, r is the distance between the interaction centres and ε and r_0 represent the interaction well depth and equilibrium distance, respectively. When

effective atoms are considered, ε and r_0 are directly obtained from basic physical properties of the interaction centres. In our case we have the $\text{K}^+\text{-H}_2\text{O}$, $\text{Na}^+\text{-H}_2\text{O}$ and $\text{H}_2\text{O}\text{-H}_2\text{O}$ pairs. The interaction centres are placed on the cation and on the oxygen atom of the water molecule and ε and r_0 are calculated from the polarisability and charge of the potassium and sodium ions and the average polarisability of water [44].

A key feature of the ILJ function (Eq. 2) is the additional β parameter, that corrects most of the inadequacies of the well known Buckingham (exp,6) and Lennard Jones (LJ) models [40], for which alternative forms have yet been proposed [45]. The proposed alternative models, in fact, although satisfactorily reproducing the mid-range features of the potential well, fail in describing accurately both the short-range repulsion and the long-range attraction. Moreover, the introduction of the parameter β , of the ILJ model by allowing the portable use of the same values of ε and r_0 for the same interactions centres in different environments, adds the necessary flexibility to the V_{ILJ} function in comparison with the V_{LJ} one [46]. A wise use of β (the only adjustable parameter in Eq. 2), permits to incorporate some additional effects, for instance charge transfer, in an effective way [47]. The parameter m is set equal to 4 or 6 to describe ion-neutral and neutral-neutral interactions, respectively. The parameters ε , r_0 and β adopted for $\text{K}^+\text{-H}_2\text{O}$, $\text{Na}^+\text{-H}_2\text{O}$ and $\text{H}_2\text{O}\text{-H}_2\text{O}$ interaction pairs are reported in Table 1.

Table 1. Values of well depth (ε), equilibrium distance (r_0) and parameter β defining the $\text{K}^+\text{-H}_2\text{O}$, $\text{Na}^+\text{-H}_2\text{O}$ and $\text{H}_2\text{O}\text{-H}_2\text{O}$ non electrostatic energy contributions

	ε / meV	r_0 / Å	β
$\text{K}^+\text{-(H}_2\text{O)}$	102.10	3.161	7.0
$\text{Na}^+\text{-(H}_2\text{O)}$	151.89	2.732	6.0
$\text{(H}_2\text{O)}\text{-(H}_2\text{O)}$	9.060	3.730	7.5

The electrostatic interaction contributions contained in each term of Eq. 1 are calculated by placing on any single water molecule a set of point charge whose distribution reproduces the H_2O dipole and quadrupole moments and by applying to them the Coulomb law.

It is important to mention here that the dipole moment of the H_2O monomer has been again considered only as an effective model parameter, related to the true dipole moment of H_2O in the ionic aggregate but not necessarily coincident with it. The parameterization of the $\text{H}_2\text{O}\text{-H}_2\text{O}$ non electrostatic interaction contribution was performed using scaling laws exploiting the overall molecular polarizability. The electrostatic charge distribution for the dimer was derived from its dipole moment, equal to 2.1 D [48]. The potential energy function allows to obtain second virial coefficients in excellent agreement with experimental results [49]. By using the same parameters of the potential and only increasing slightly the dipole moment of the monomer, radial distribution functions were calculated for both rigid and flexible ensembles.

As a matter of fact, in our simulations the values 2.1 and 2.07 D (for Na^+ and K^+ , respectively) have been used in order to best reproduce the information available from the literature [50]. To reproduce the dipole moment of the water molecules we placed charges of -0.74726 a.u. and -0.7366 a.u. on the O atom and of 0.37363 and 0.3683 a.u. on the H atoms for Na^+ and K^+ in solution, respectively. We have considered [51] the OH bond distances as equal to 1.00 Å and the HOH angle as equal to 109.47 degrees.

The water molecules in simulations have been considered flexible using an harmonic potential function to describes the dependence of the internal molecular potential energy on the atom displacements from the equilibrium positions, for each mode of vibration. In this case, the intramolecular potential functions for the flexible water are given for the bond and angle interactions by a harmonic model potential.

3 Molecular Dynamics: Calculations

3.1 The Simulation Protocol

Classical molecular dynamics simulations were performed using the DL_POLY [52] molecular dynamics simulation package. We performed classical MD simulations of $\text{M}^+(\text{H}_2\text{O})_n$, $n = 3 - 8$, using structures optimized by means of ab initio calculations, (DFT/B3LYP method) taken from literature [21] for both ions. For each optimized structure, we performed simulations with increasing temperature. A microcanonical ensemble (NVE) of particles, where the number of particles, N, volume, V, and total energy, E, are conserved, has been considered. The total energy, E, is expressed as a sum of potential and kinetic energies. The first one is decomposed in non electrostatic and electrostatic contributions and its mean value at the end of the trajectory is represented by the average configuration energy E_{cfg} ($E_{cfg} = E_{nel} + E_{el}$). The kinetic energy at each step, E_{kin} , allows to determine the instantaneous temperature, T, whose mean values can be calculated at the end of the simulation. The total time interval for each simulation trajectory was set equal to 2 ns after equilibration at each temperature. We implemented the Improved Lennard-Jones potential function and used it and used it to treat all the intermolecular interactions in $\text{M}^+(\text{H}_2\text{O})_n$, $n = 3 - 8$. For each ion, statistical data were collected for 2 ns production run. The hydration system consists of flexible water molecules (bond and angle vibrations). This simulation time is sufficiently long to allow observation of isomerisation processes and fragmentation of both ions-water clusters. Most of the calculations have been performed at values of total energy that correspond to the 10 K-100 K temperature range. A specific value of T can be achieved by allowing a temperature equilibration of the system, with the corresponding results excluded in the statistical analysis performed at the end of the trajectory. The behavior of the aggregates has been investigated at low and high temperatures. At low temperatures, if the system is not far from the equilibrium configuration, the energy value obtained from an extrapolation at $T = 0$ K should be close to that at equilibrium and the corresponding configurations can be considered as

equilibrium-like structures. By increasing T , other configurations far away from equilibrium can be reached and the system can surmount isomerisation barriers.

The dynamics simulations reveal interesting features in the isomerization of the ion-water cluster structures. We report here results on the thermal stability and dynamical behavior of the K^+ and Na^+ water clusters classical molecular dynamics.

3.2 The Potassium-Water Clusters $K^+-(H_2O)_n$ ($n=3 - 8$)

The K^+-H_2O interaction was previously tested by performing MD simulations of ionic water solutions, for which the same ILJ parameters but different charge distribution (derived from the dipole moment of bulk water) was used [37].

From the structures optimized by ab initio calculation (see Fig. 1), (DFT/B3LYP method) we observed the isomerization of the $[K(H_2O)_3]^+$ cluster from a structure with symmetry (C_{2v}) to one with symmetry (D_3), displacing one of the water molecules from a longer distance of 4.5 Å (from the second hydration shell) a shorter one by placing K^+ at the bond distance of 2.75 Å (first hydration shell), after 1.27 ns, (see Fig. 2 reporting the evolution of K^+-O bond

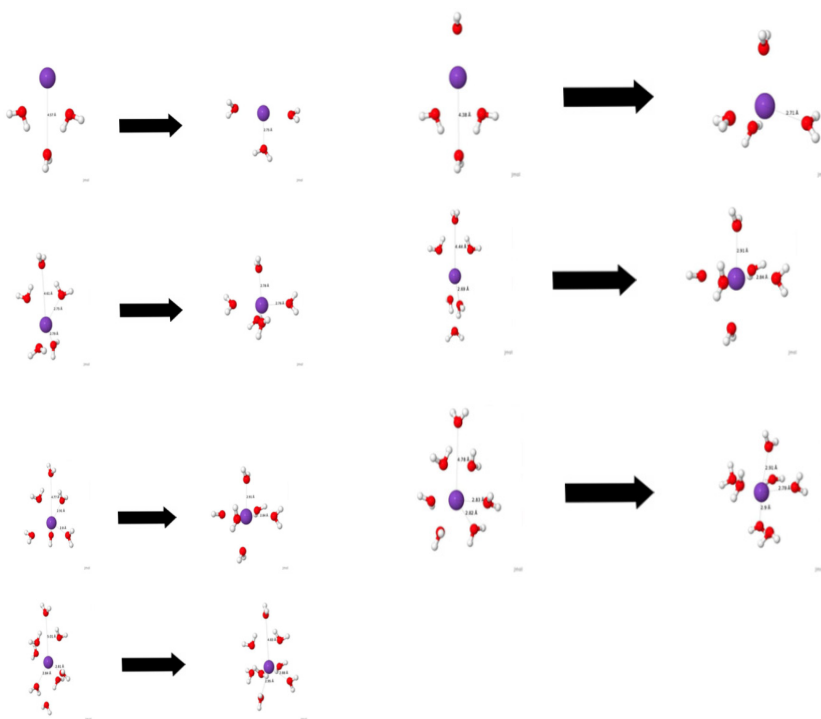


Fig. 1. $[K-(H_2O)_n]^+$ ($n=3 - 8$) initial and final isomerization structures. (See Sec. 3.2)

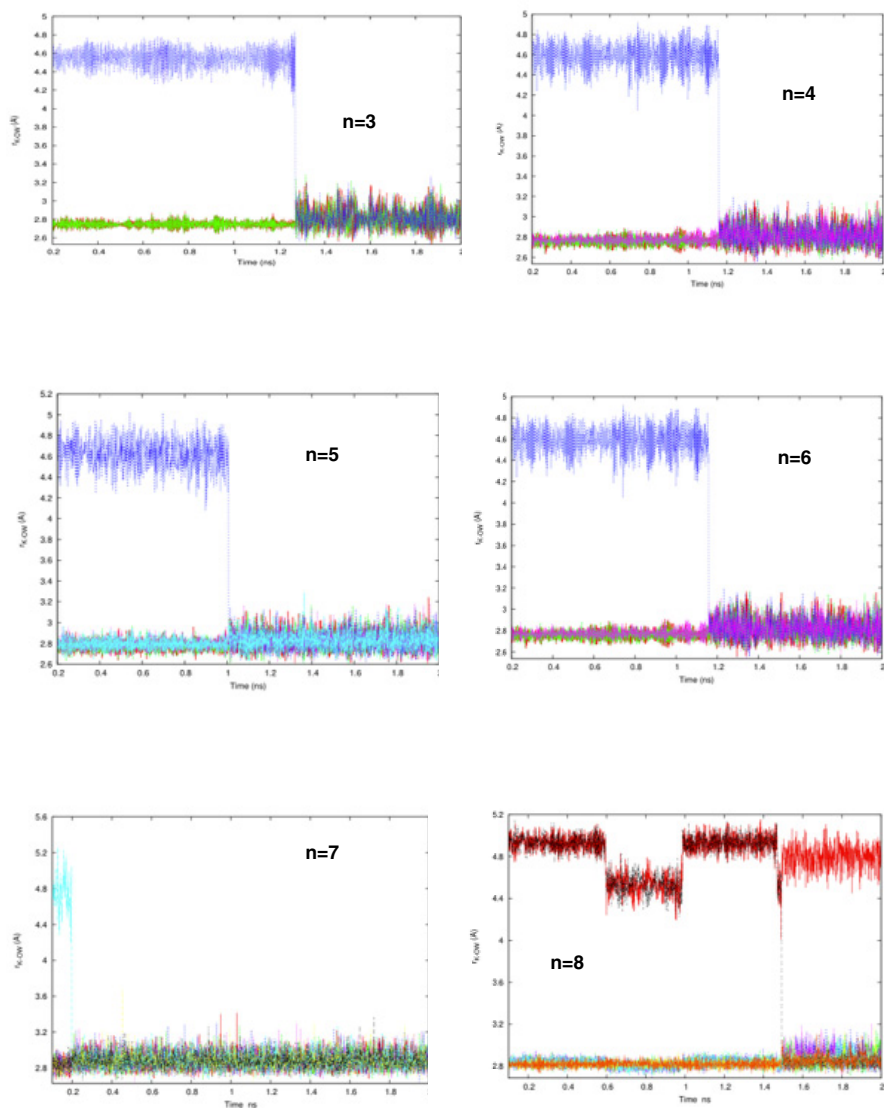
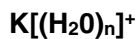


Fig. 2. Time evolution of the distance from K^+ to the O atom of H_2O for the $[\text{K}-(\text{H}_2\text{O})_n]^+$ ($n=3-8$) clusters at different values of the temperature T (different molecules are represented by different colours).

distance during the simulation). MD simulations at 50 K of the $[\text{K}(\text{H}_2\text{O})_n]^+$ cluster have been run using as initial configuration a C_2 one obtained from DFT calculations [21]. An isomerization from the initial C_2 symmetry structure to a S_4 symmetry structure has been observed, consisting in a displacement of a water molecule from a distance of 4.6 Å from the K^+ atom (typical of the second hydration shell) to a distance of 2.8 Å (characteristic of the first hydration shell (see [11])). The isomerization occurs after 1.16 ns. The time evolution of the K^+ -O distance that reveals the isomerization is shown in Fig. 2. Due to the lower configurational energy of the S_4 structure, the cluster has a higher temperature after isomerization (see Fig. 5).

Fig. 1, too, shows the isomerization of the $[\text{K}(\text{H}_2\text{O})_5]^+$ cluster from the structure with symmetry (C_2) to one with a structure of the same symmetry. This follows a displacement of one of the water molecules from a distance of 4.6 Å from the K^+ atom to a distance of 2.8 Å, by reporting the time evolution of the K^+ -O distance during the simulation of the cluster performed at 60 K. The isomerization occurs after 1 ns and is accompanied by a temperature increase to higher values due to the occupation of another minimum on the PES with lower configurational energy. For the $[\text{K}(\text{H}_2\text{O})_6]^+$ cluster, two isomerizations were found from two different initial structures. The first one, shows the transition from the structure with symmetry (C_2) to the one with symmetry (C_4) by the displacement of two water molecules from a distance of 4.45 Å (second hydration shell) from K^+ to a distance of 2.85 Å (first hydration shell), as shown by the time evolution of the K^+ -O bond distance in Fig. 2. The second kind of isomerization is given by a transition from the structure with symmetry (C_1) to the one with symmetry (C_4) through the displacement of one of the

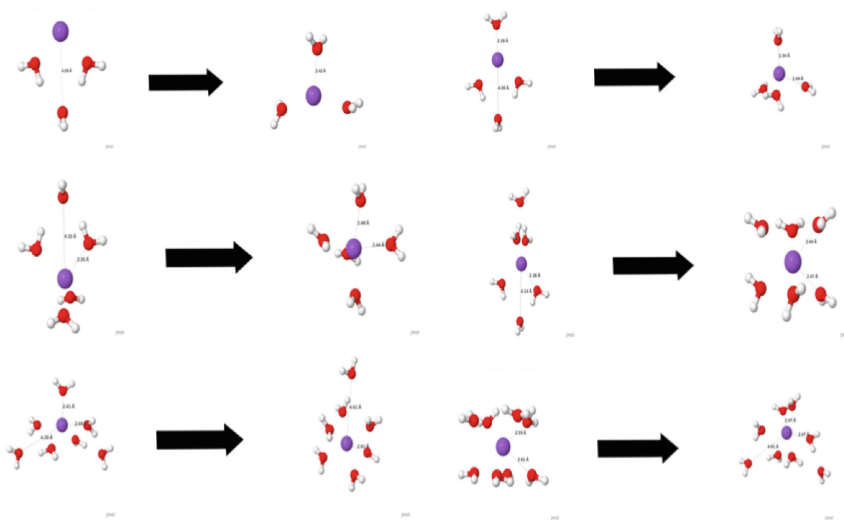


Fig. 3. $[\text{Na}-(\text{H}_2\text{O})_n]^+$ ($n=3 - 8$) initial and final isomerization structures. (See Sec. 3.3)

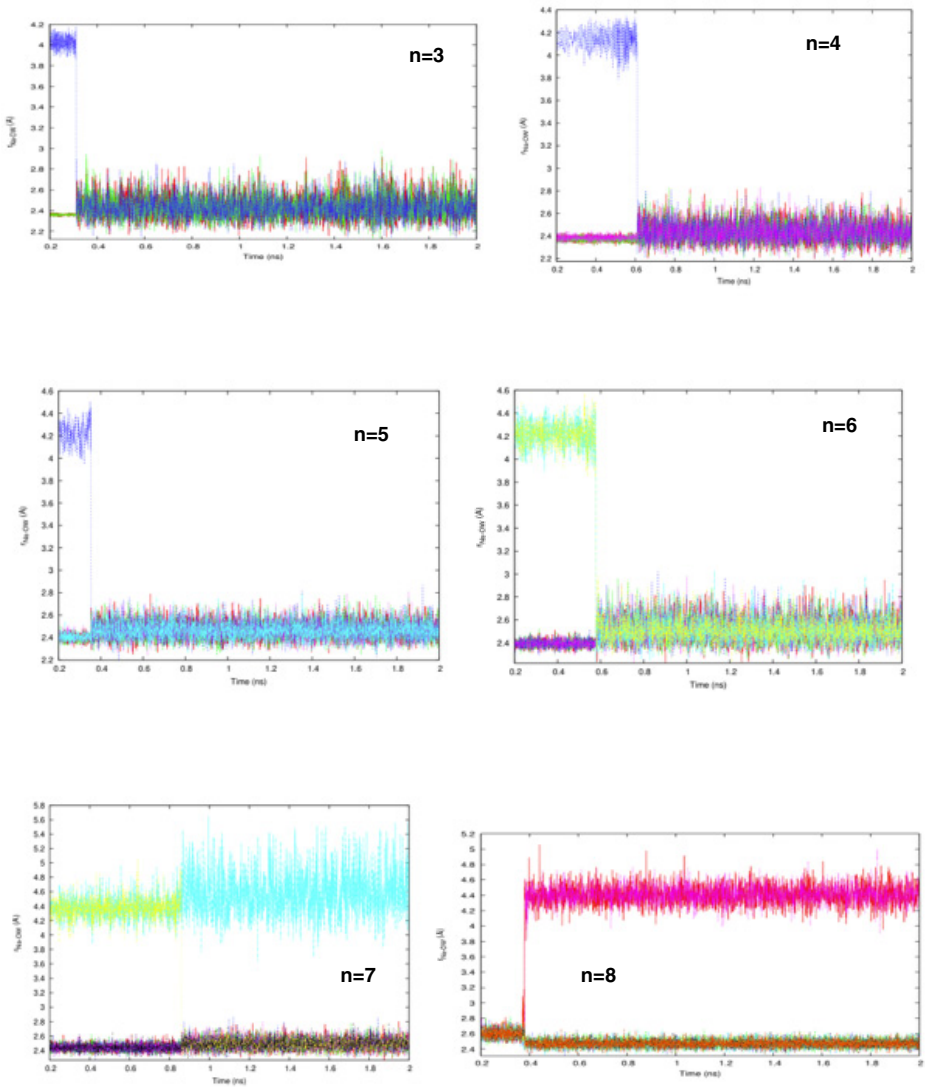
$\text{Na}[(\text{H}_2\text{O})_n]^+$ 

Fig. 4. Evolution of the distance from Na^+ to the O atom of H_2O for the $[\text{Na}-(\text{H}_2\text{O})_n]^+$ ($n=3-8$) at different values of T (different molecules are represented by different colours).

water molecules from a longer distance of 4.8 Å (second hydration shell) from K^+ to a distance of 2.85 Å (first hydration shell). These isomerizations occur in the simulations performed at 25 and 80 K, respectively, and correspond to a temperature increase to higher values due to the occupation of minima on the PES with lower configurational energy. The transitions occur after 1.36 ns and 0.55 ns (see Figs. 1 and 2) respectively. The $[K(H_2O)_7]^+$ cluster undergoes isomerization from the structure with symmetry (C_2) to another structure with the same symmetry, following the displacement of one of the water molecules from a distance of 4.8 Å (second hydration shell) from K^+ to a distance of 2.9 Å (first hydration shell), as shown in the time evolution of the K^+ -O distance reported in Fig. 2. This isomerization occurs after 0.02 ns in the simulation performed at 75 K with a temperature increase to higher values due to the occupation of another minimum on the PES with lower configurational energy. Finally, for the cluster $[K(H_2O)_8]^+$, a transition from the structure with symmetry (C_2) to the one with symmetry of (C_1) through the displacement of one of the water molecules from a distance of 5 Å from K^+ to a distance of 2.9 Å is shown in Fig. 2 the time evolution of the K^+ -O distance. This isomerization occurs in the simulation performed at 15 K with a temperature increase to higher values due to the occupation of another minimum on the PES with lower configurational energy, after 1.5 ns.

These isomerization processes occur in the simulation performed at $T=$ 25, 35, 50, 60, 75 and 80 K as initial temperature for the $K^+-(H_2O)_n$ with $n=3-8$, respectively. The initial structure transformed into a more stable one by reaching another energy minimum of the potential energy surface with a lower potential energy (see Fig. 2, where the time evolution of the configurational energy during the simulation is shown).

3.3 Sodium-Water Clusters $Na^+-(H_2O)_n$ ($n=3-8$)

Fig. 3 shows the structure transformation in the $[Na(H_2O)_3]^+$ cluster from the structure with symmetry (C_{2v}) to the one with symmetry (D_3) through the displacement of one of the water molecules from longer distance 4.1 Å (from the second hydration shell) the Na^+ with a bond distance of 2.4 Å (the first hydration shell) after 0.31 ns simulation (as shown in Fig. 4 following the evolution of the Na^+ -O bond distance).

This isomerization occurs in the simulation with an initial temperature of 15 K. The initial structure was transformed into a more stable corresponding to another energy minimum in the potential energy surface with a lower potential energy while the total energy is constant (due to the use of the NVE ensemble which conserve the total energy), the same behaviour as discussed for K^+ . When, adding one more molecule of water, the $[Na(H_2O)_4]^+$ cluster transform from a structure with symmetry (C_2) to the one with symmetry (S_4) through the displacement of one of the water molecules from longer distance 4.1 Å (second hydration shell) Na^+ with a bond distance of 2.4 Å (first hydration shell) after 0.61 ns (as shown in Fig. 4 by the time evolution of the Na^+ -O bond distance).

This isomerization occurs in the simulation performed at 25 K with a temperature jump to higher values due to the occupation of another minimum on the PES with lower configurational energy at 0.61 ns. For the structure transformation in the $[\text{Na}(\text{H}_2\text{O})_5]^+$ cluster from the structure with symmetry (C_2) to the other with symmetry (S_3) through the displacement of two water molecules from longer distance 4.1 Å (second hydration shell) Na^+ with bond distance 2.4 Å (first hydration shell). In this case the isomerization occurs at 40 K and 0.58 ns. Unlike to the K^+ -water clusters in the case of the $[\text{Na}(\text{H}_2\text{O})_6]^+$ one we found only one isomerization. The aggregate structure passes from a structure with symmetry (C_2) to the one with symmetry (S_3) including the displacement of one of the water molecules from the longer distance of 4.4 Å (second hydration shell) the Na^+ with bond distance 2.4 Å (first hydration shell) at 40 K well before the reach 1/2 ns of the simulation. The structure transformation in the $[\text{Na}(\text{H}_2\text{O})_7]^+$ cluster from the structure with symmetry (C_2) to the other with symmetry (C_1) taking account of the displacement of one water molecules from longer distance 4.4 Å (second hydration shell) the Na^+ with a bond distance of 2.4 Å (first hydration shell) at 70 K and before 1 ns. Meanwhile, we observed the displacement of two of the water molecules from shorter distance 2.6 Å (first hydration shell) away from the Na^+ with a bond distance of 4.4 Å (second hydration shell) while the other six bonds move to slightly shorter distance contracting the radius of the first shell to 2.5 Å for the $[\text{Na}(\text{H}_2\text{O})_8]^+$ cluster. That is indicating the tendency of the first shell to dissociate reducing to only six water molecules in agreement with the coordination numbers obtained from the classical MD calculation of Na^+ in liquid water. This isomerization occurs in the simulation performed at 35 K and very fast, at 0.38 ns of the simulation. All, the behaviours can be observed in the Figs. 3 and 4.

4 Conclusions

Our MD calculations have focused on the investigation on whether the Improved Lennard-Jones potential is suited to accurately simulate the K^+ and Na^+ water cluster dynamics and structures by matching the stable structures predicted by DFT calculations as a results of the evolution over PES through the isomerization. We have found, indeed, that, under the considered conditions, the $[\text{Na}(\text{H}_2\text{O})_8]^+$ cluster tends to dissociate from a one shell structure to a two shell structure with coordination number 6 because of the smaller size of the Na^+ ion with respect to that of K^+ . In addition, we have been able to estimate the temperature effect of the isomerization between these two different structures by progressively adding a water molecule to the initial $[\text{K}(\text{H}_2\text{O})_n]^+$ and $[\text{Na}(\text{H}_2\text{O})_n]^+$ clusters as nicely confirmed by Fig. 5 that shows the change of the isomerization temperature in $[\text{K}(\text{H}_2\text{O})_n]^+$ and $[\text{Na}(\text{H}_2\text{O})_n]^+$ clusters by increasing of the number of water molecules (n). As a matter of fact, the figure, shows that for K^+ , the isomerization temperature increases until $n=6$ indicating more configurational energy released and converted to kinetic energy heating the system, and, after that, the temperature starts decreasing meaning less released

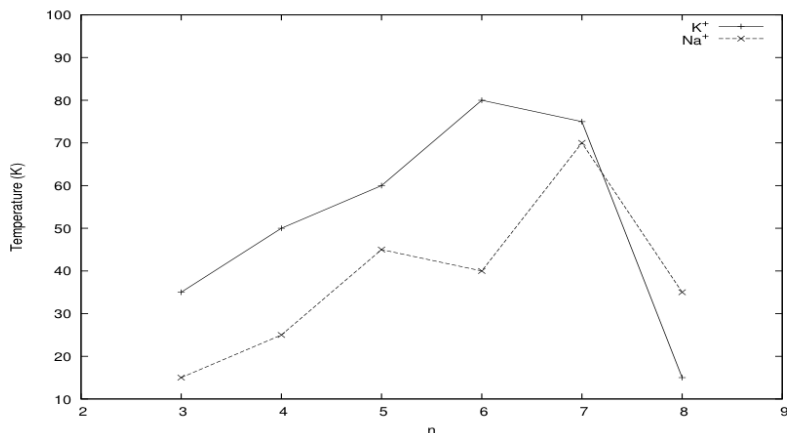


Fig. 5. Isomerization temperature as a function of the number of water molecules (n) in $[\text{K}(\text{H}_2\text{O})_n]^+$ and $[\text{Na}(\text{H}_2\text{O})_n]^+$ clusters

energy, and less energy gained. The higher energy jump occurs at $n=6$, around the calculated coordination number in the K^+ water liquid system, while in the case of the Na^+ the isomerization temperature increases until $n=5$ indicating more configurational energy released and moving to more stable structures. The temperature for Na^+ at $n=6$ is almost the same at $n=5$ indicating that the most stable structure is one of these two structures. After that, for higher n values we have seen the tendency of the $[\text{Na}(\text{H}_2\text{O})_8]^+$ complex to shrink the first hydration shell to 6 water molecules and release the other two water molecules to the second hydration shell.

Acknowledgments. M. Albertí acknowledges financial support from the Ministerio de Educación y Ciencia (Spain, Projects CTQ2013-41307-P) and to the Comissionat per a Universitats i Recerca del DIUE (Generalitat de Catalunya, Project 201456R25). The Centre de Serveis Científics i Acadèmics de Catalunya CESA and Fundació Catalana per a la Recerca are also acknowledged for the allocated supercomputing time. Noelia Faginas Lago acknowledges financial support from MIUR PRIN 2008 (contract 2008KJX4SN 003), Phys4entry FP72007-2013 (contract 242311). The computing for this project was performed at the OU Supercomputing Center for Education & Research (OSCER) at the University of Oklahoma (OU). A. Lombardi also acknowledges financial support to MIUR-PRIN 2010-2011 (contract 2010ERFKXL 002). Thanks are also due to INSTM, IGI and the COMPCHEM virtual organization for the allocation of computing time.

References

1. Dunand, F., Helm, L., Merbach, A.: Solvent exchange on metal ions. *Advances in Inorganic Chemistry* **54**, 1–69 (2003)
2. Helm, L., Merbach, A.E.: Applications of advanced experimental techniques: high pressure nmr and computer simulations. *J. Chem. Soc., Dalton Trans.* **5**, 633–641 (2002)

3. Helm, L., Merbach, A.E.: Inorganic and bioinorganic solvent exchange mechanisms. *Chemical Reviews* **105**, 1923–1960 (2005). PMID: 15941206
4. Helm, L., Nicolle, G.M., Merbach, A.E.: Water and proton exchanges processes on metal ions. *Adv. Inorg. Chem.* **57**, 327–379 (2005)
5. Lincoln, S.F., Merbach, A.E.: Substitution reactions of solvated metal ions. **42**, 1–88 (1995)
6. Marcus, Y.: Effect of ions on the structure of water: Structure making and breaking. *Chemical Reviews* **109**, 1346–1370 (2009). PMID: 19236019
7. Doyle, D.A., Cabral, J.M., Pfuetzner, R.A., Kuo, A., Gulbis, J.M., Cohen, S.L., Chait, B.T., MacKinnon, R.: The structure of the potassium channel: Molecular basis of k⁺ conduction and selectivity. *Science* **280**, 69–77 (1998)
8. Guidoni, L., Torre, V., Carloni, P.: Potassium and sodium binding to the outer mouth of the k⁺ channel. *Biochemistry* **38**, 8599–8604 (1999). PMID: 10393534
9. Laio, A., Torre, V.: Physical origin of selectivity in ionic channels of biological membranes. *Biophysical Journal* **76**, 129–148 (1999)
10. Mooney, B.L., Corrales, L.R., Clark, A.E.: Novel analysis of cation solvation using a graph theoretic approach. *The Journal of Physical Chemistry B* **116**, 4263–4275 (2012). PMID: 22417120
11. Faginas-Lago, N., Lombardi, A., Albertí, M., Grossi, G.: Accurate analytic intermolecular potential for the simulation of na⁺ and k⁺ ion hydration in liquid water. *Journal of Molecular Liquids* **204**, 192–197 (2015)
12. Neilson, G.W., Mason, P.E., Ramos, S., Sullivan, D.: Neutron and x-ray scattering studies of hydration in aqueous solutions. *Philosophical Transactions of the Royal Society of London A: Mathematical, Physical and Engineering Sciences* **359**, 1575–1591 (2001)
13. Soper, A.K., Weckström, K.: Ion solvation and water structure in potassium halide aqueous solutions. *Biophysical Chemistry* **124**(3), 180–191 (2006). <http://www.sciencedirect.com/science/article/pii/S0301462206001207>
14. Glezakou, V.A., Chen, Y., Fulton, J., Schenter, G., Dang, L.: Electronic structure, statistical mechanical simulations, and exafs spectroscopy of aqueous potassium. *Theoretical Chemistry Accounts* **115**, 86–99 (2006)
15. Varma, S., Rempe, S.B.: Coordination numbers of alkali metal ions in aqueous solutions. *Biophysical Chemistry* **124**, 192–199 (2006). Ion Hydration Special Issue
16. Caminiti, R., Licheri, G., Paschina, G., Piccaluga, G., Pinna, G.: Interactions and structure in aqueous nano3 solutions. *The Journal of Chemical Physics* **72**, 4522–4528 (1980)
17. Skipper, N.T., Neilson, G.W.: X-ray and neutron diffraction studies on concentrated aqueous solutions of sodium nitrate and silver nitrate. *J. Phys. Condens. Matter* **1**, 4141–4154 (1989)
18. Michaelian, K.H., Moskovits, M.: Tetrahedral hydration of ions in solution. *Nature* **273**, 135–136 (1978)
19. Ohtaki, H., Radnai, T.: Structure and dynamics of hydrated ions. *Chemical Reviews* **93**, 1157–1204 (1993)
20. Köpfer, D.A., Song, C., Gruene, T., Sheldrick, G.M., Zachariae, U., de Groot, B.L.: Ion permeation in k⁺ channels occurs by direct coulomb knock-on. *Science* **346**, 352–355 (2014)
21. Shafei, R.A.M.: Theoretical Study of Ion Water Interaction Ab Initio and Classical Molecular Dynamics, September 2014
22. Pirani, F., Cappelletti, D., Liuti, G.: Range, strength and anisotropy of intermolecular forces in atom-molecule systems: an atom-bond pairwise additivity approach. *Chem. Phys. Lett.* **350**, 286–296 (2001)

23. Albertí, M., Castro, A., Laganà, A., Pirani, F., Porrini, M., Cappelletti, D.: Properties of an atom-bond additive representation of the interaction for benzene-argon clusters. *Chemical Physics Letters* **392**, 514–520 (2004)
24. Bartolomei, M., Pirani, F., Lagan, A., Lombardi, A.: A full dimensional grid empowered simulation of the $\text{CO}_2 + \text{CO}_2$ processes. *Journal of Computational Chemistry* **33**, 1806–1819 (2012)
25. Lombardi, A., Faginas-Lago, N., Pacifici, L., Costantini, A.: Modeling of energy transfer from vibrationally excited CO_2 molecules: Cross sections and probabilities for kinetic modeling of atmospheres, flows, and plasmas. *J. Phys. Chem. A* **117**, 11430–11440 (2013)
26. Lago, N.F., Albertí, M., Laganà, A., Lombardi, A., Pacifici, L., Costantini, A.: The molecular stirrer catalytic effect in methane ice formation. In: Murgante, B., Misra, S., Rocha, A.M.A.C., Torre, C., Rocha, J.G., Falcão, M.I., Taniar, D., Apduhan, B.O., Gervasi, O. (eds.) ICCSA 2014, Part I. LNCS, vol. 8579, pp. 585–600. Springer, Heidelberg (2014)
27. Lombardi, A., Laganà, A., Pirani, F., Palazzetti, F., Lago, N.F.: Carbon oxides in gas flows and earth and planetary atmospheres: state-to-state simulations of energy transfer and dissociation reactions. In: Murgante, B., Misra, S., Carlini, M., Torre, C.M., Nguyen, H.-Q., Taniar, D., Apduhan, B.O., Gervasi, O. (eds.) ICCSA 2013, Part II. LNCS, vol. 7972, pp. 17–31. Springer, Heidelberg (2013)
28. Falcinelli, S., Rosi, M., Candori, P., Vecchiocattivi, F., Bartocci, A., Lombardi, A., Lago, N.F., Pirani, F.: Modeling the intermolecular interactions and characterization of the dynamics of collisional autoionization processes. In: Murgante, B., Misra, S., Carlini, M., Torre, C.M., Nguyen, H.-Q., Taniar, D., Apduhan, B.O., Gervasi, O. (eds.) ICCSA 2013, Part I. LNCS, vol. 7971, pp. 69–83. Springer, Heidelberg (2013)
29. Lombardi, A., Lago, N.F., Laganà, A., Pirani, F., Falcinelli, S.: A bond-bond portable approach to intermolecular interactions: simulations for N-methylacetamide and carbon dioxide dimers. In: Murgante, B., Gervasi, O., Misra, S., Nedjah, N., Rocha, A.M.A.C., Taniar, D., Apduhan, B.O. (eds.) ICCSA 2012, Part I. LNCS, vol. 7333, pp. 387–400. Springer, Heidelberg (2012)
30. Laganà, A., Lombardi, A., Pirani, F., Gamallo, P., Sayos, R., Armenise, I., Cacciatore, M., Esposito, F., Rutigliano, M.: Molecular physics of elementary processes relevant to hypersonics: atom-molecule, molecule-molecule and atom-surface processes. *The Open Plasma Physics Journal* **7**, 48 (2014)
31. Faginas-Lago, N., Albertí, M., Costantini, A., Laganà, A., Lombardi, A., Pacifici, L.: An innovative synergistic grid approach to the computational study of protein aggregation mechanisms. *Journal of Molecular Modeling* **20**, 2226 (2014)
32. Albert, M., Castro, A., Lagan, A., Moix, M., Pirani, F., Cappelletti, D., Liuti, G.: A molecular dynamics investigation of rare-gas solvated cation-benzene clusters using a new model potential. *The Journal of Physical Chemistry A* **109**, 2906–2911 (2005). PMID: 16833608
33. Albertí, M., Aguilar, A., Lucas, J., Pirani, F.: Static and dynamic properties of anionic intermolecular aggregates: the i-benzene- Ar_n case. *Theoretical Chemistry Accounts* **123**, 21–27 (2009)
34. Faginas-Lago, N., Albertí, M., Laganà, A., Lombardi, A.: Water $(\text{H}_2\text{O})_m$ or benzene $(\text{C}_6\text{H}_6)_n$ Aggregates to Solvate the K^+ ? In: Murgante, B., Misra, S., Carlini, M., Torre, C.M., Nguyen, H.-Q., Taniar, D., Apduhan, B.O., Gervasi, O. (eds.) ICCSA 2013, Part I. LNCS, vol. 7971, pp. 1–15. Springer, Heidelberg (2013)

35. Albertí, M.: Rare gas-benzene-rare gas interactions: Structural properties and dynamic behavior. *The Journal of Physical Chemistry A* **114**, 2266–2274 (2010). PMID: 20104928
36. Albertí, M., Aguilar, A., Lucas, J.M., Pirani, F., Cappelletti, D., Coletti, C., Re, N.: Atom-bond pairwise additive representation for cation-benzene potential energy surfaces: An ab initio validation study. *The Journal of Physical Chemistry A* **110**, 9002–9010 (2006). PMID: 16836464
37. Coletti, C., Re, N.: Theoretical study of alkali cation-benzene complexes: Potential energy surfaces and binding energies with improved results for rubidium and cesium. *J. Phys. Chem. A* **110**, 6563 (2006)
38. Liuti, G., Pirani, F.: Regularities in van der waals forces: correlation between the potential parameters and polarizability. *Chem. Phys. Lett.* **122**, 245 (1985)
39. Albertí, M., Lago, N.F.: Competitive solvation of K^+ by C_6H_6 and H_2O in the $K^+-(C_6H_6)_n-(H_2O)_m$ ($n = 1-4$; $m = 1-6$) aggregates. *European Physical Journal D* **67**(4), art. no. 73 (2013). <http://www.scopus.com/inward/record.url?eid=2-s2.0-84879071541&partnerID=40&md5=d471977fe0c15ea412f5330514ec038c>
40. Pirani, F., Albertí, M., Castro, A., Moix, M., Cappelletti, D.: Atom-bond pairwise additive representation for intermolecular potential energy surfaces. *Chem. Phys. Lett.* **394**, 37 (2004)
41. Pirani, P., Brizi, S., Roncaratti, L., Casavecchia, P., Cappelletti, D., Vecchiocattivi, F.: Beyond the lennard-jones model: a simple and accurate potential function probed by high resolution scattering data useful for molecular dynamics simulations. *Phys. Chem. Chem. Phys.* **10**, 5489 (2008)
42. Albertí, M., Faginas-Lago, N., Laganà, A., Pirani, F.: A portable intermolecular potential for molecular dynamics studies of nma-nma and nma-h₂o aggregates. *Phys. Chem. Chem. Phys.* **13**, 8422–8432 (2011)
43. Albertí, M., Aguilar, A., Lucas, J.M., Pirani, F., Coletti, C., Re, N.: Atom-bond pairwise additive representation for halide-benzene potential energy surfaces: an ab initio validation study. *J. Phys. Chem. A* **113**, 14606 (2009)
44. Albertí, M., Aguilar, A., Cappelletti, D., Laganà, A., Pirani, F.: On the development of an effective model potential to describe ater interaction in neutral and ionic clusters. *Int. J. Mass Spec.* **280**, 50–56 (2009)
45. Halgren, T.A.: The representation of van der waals (vdw) interactions in molecular mechanics force fields: potential form, combination rules, and vdw parameters. *J. Am. Chem. Soc.* **114**, 7827 (1992)
46. Albertí, M., Aguilar, A., Lucas, J.M., Pirani, F.: A generalized formulation of ion-electron interactions: Role of the nonelectrostatic component and probe of the potential parameter transferability. *J. Phys. Chem. A* **114**, 11964–11970 (2010)
47. Albertí, M., Aguilar, A., Lucas, J.M., Pirani, F.: Competitive role of ch_4 - $ch_{xi}4$ and ch - π interactions in c_6h_6 - $(ch_4)_n$ aggregates: The transition from dimer to cluster features. *The Journal of Physical Chemistry A* **116**, 5480–5490 (2012). PMID: 22591040
48. Gregory, J.K., Clary, D.C., Liu, K., Brown, M.G., Saykally, R.J.: **275**, 814 (1997)
49. Albertí, M., Aguilar, A., Bartolomei, M., Cappelletti, D., Laganà, A., Lucas, J., Pirani, F.: A study to improve the van der waals component of the interaction in water clusters. *Phys. Script.* **78**, 058108 (2008)

50. Ikeda, T., Boero, M., Terakura, K.: *J. Chem. Phys.* **126**, 034801 (2007)
51. Manion, J.A., Huie, R.E., Levin Jr., R.D., D.R.B., Orkin, V.L., Tsang, W., McGivern, W.S., Hudgens, J.W., Knyazev, V.D., Atkinson, D.B., Chai, E., Tereza, A.M., Lin, C.Y., Allison, T.C., Mallard, W.G., Westley, F., Herron, J.T., Hampson, R.F., Frizzell, D.H.: *Nist chemical kinetics database, nist standard reference database 17* (2013)
52. Smith, W., Yong, C., Rodger, P.: *DL_poly: Application to molecular simulation. Molecular Simulation* **28**, 385–471 (2002)